

Resonant inelastic x-ray scattering study of charge excitations in superconducting and nonsuperconducting PrFeAsO_{1-y}

I. Jarrige,^{1,2,*} T. Nomura,^{1,2} K. Ishii,^{1,2} H. Gretarsson,³ Y.-J. Kim,³ J. Kim,⁴ M. Upton,⁴ D. Casa,⁴ T. Gog,⁴ M. Ishikado,^{2,5,†} T. Fukuda,^{1,2} M. Yoshida,¹ J. P. Hill,⁶ X. Liu,⁶ N. Hiraoka,⁷ K. D. Tsuei,⁷ and S. Shamoto^{2,5}

¹Japan Atomic Energy Agency, SPring-8, 1-1-1 Kouto, Sayo, Hyogo 679-5148, Japan

²JST, TRIP, 5, Sanbancho, Chiyoda, Tokyo 102-0075, Japan

³Department of Physics, University of Toronto, Toronto, Ontario M5S 1A7, Canada

⁴Advanced Photon Source, Argonne National Laboratory, Argonne, Illinois 60439, USA

⁵Quantum Beam Science Directorate, Japan Atomic Energy Agency, Tokai, Ibaraki 319-1195, Japan

⁶Department of Condensed Matter Physics and Materials Science, Brookhaven National Laboratory, Upton, New York 11973, USA

⁷National Synchrotron Radiation Research Center, Hsinchu 30076, Taiwan

(Received 13 March 2012; revised manuscript received 17 August 2012; published 5 September 2012)

We report the first observation by momentum-resolved resonant inelastic x-ray scattering of charge excitations in an iron-based superconductor and its parent compound, $\text{PrFeAsO}_{0.7}$ and PrFeAsO , respectively, with two main results. First, using calculations based on a 16-band dp model, we show that the energy of the lowest-lying excitations, identified as dd interband transitions of dominant xz, yz orbital character, exhibits a dramatic dependence on electron correlation. This enables us to estimate the Coulomb repulsion U and Hund's coupling J , and to highlight the role played by J in these peculiar orbital-dependent electron correlation effects. Second, we show that short-range antiferromagnetic correlations, which are a prerequisite to the occurrence of these excitations at the Γ point, are still present in the superconducting state.

DOI: [10.1103/PhysRevB.86.115104](https://doi.org/10.1103/PhysRevB.86.115104)

PACS number(s): 74.25.Jb, 74.62.-c, 74.70.Xa, 78.70.Ck

Not only has high- T_c superconductivity in the iron pnictides become one of the fastest-flourishing topics in recent condensed matter physics, but the extensive research effort it has generated has not abated to date. At the heart of this persistent interest lies the sharp contrast with the electronic properties of the strongly correlated, insulating, high- T_c cuprates, since the pnictides are metallic, albeit with sizable correlations. Another distinctive aspect of the pnictides is the multi-orbital nature of their low-energy electronic structure, which drives complex many-body interactions. In particular, the central role played by Hund's rule coupling J was recently highlighted, as a theoretical consensus emerged that the electron-electron interaction in multiband materials is dictated by J rather than Coulomb U or by a nontrivial interplay of both.^{1,2}

In this context, experimental investigations of electronic excitations are invaluable in exploring the multiband electron dynamics and scrutinizing the corresponding novel theoretical frameworks. Resonant inelastic x-ray scattering (RIXS) allows such investigations to be carried out in an element-specific and momentum-resolved fashion, and in an energy range directly relevant to Coulomb and Hund interactions. However, the overwhelming fluorescence signal has been a hindering factor in the previous applications of RIXS to the pnictides.^{3,4} This Letter reports on the first successful momentum-resolved RIXS measurement of charge excitations in an iron pnictide, PrFeAsO_{1-y} , owing to both high energy resolution and good statistics. Analysis in light of theoretical calculations provides compelling insight into two key issues in pnictide physics. First, making use of the remarkable sensitivity of the low-energy, xz, yz -dominated interband transitions to electron correlation, we are able to obtain an accurate quantitative estimate of both U and J and find that J plays an important role in the orbital-dependent correlation effects. Second, our analysis discloses the presence of (at least

local) antiferromagnetic correlations in the superconducting regime.

The experiment was carried out at the MERIX endstation of the beamline 30-ID at the Advanced Photon Source. A four-bounce monochromator with asymmetrically cut Si(400) crystals yielded a bandwidth of 75 meV for the incident beam. The beam scattered from the sample was energy analyzed with a diced Ge (620) spherical analyzer and a strip detector placed on a 1-m Rowland spectrometer. A total energy resolution of 230 meV (FWHM) was achieved with this setup. The measurement was performed in the horizontal scattering geometry, with the incident photon polarization parallel to the ac plane of the tetragonal lattice [cf. Fig. 2(b)]. All measurements were performed at 10 K. Single crystals of PrFeAsO_{1-y} ($y = 0, 0.3$) were grown by a high-pressure synthesis method using a belt-type anvil apparatus described in Ref. 5. PrFeAsO_{1-y} belongs to the so-called 1111 family, which crystallizes in the ZrCuSiAs -type structure (space group $P4/nmm$). A T_c of 42 K is achieved for the optimal electron doping of $y = 0.3$.

The incident energy dependence of the RIXS spectrum measured on PrFeAsO across the Fe- K edge is shown in Fig. 1(a). The momentum was set to $(0.5, 0.5, L)$ with $L = 6.7$, which we assign to the wave vector $q = (\pi, \pi)$ as the compound has a highly two-dimensional electronic structure.⁶ The value of L is chosen so that the scattering angle is very close to 90° , which allows us to minimize the intensity of the elastic line. The maximum count rate of the RIXS signal was three counts per second, and the acquisition time for one spectrum was about 3 h. The Fe K edge is shown in Fig. 1(b), measured in the partial fluorescence yield mode by monitoring the intensity of the maximum of the $K\beta_{1,3}$ ($3p \rightarrow 1s$) emission line at 7058 eV. When varying the incident energy E_i near the maximum of the $1s \rightarrow 4p$ dipolar absorption, two weak

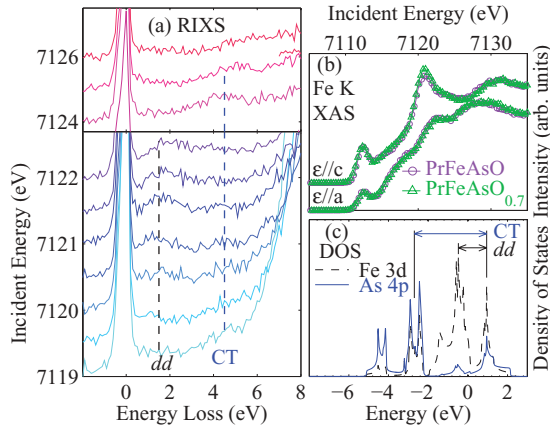


FIG. 1. (Color online) (a) Incident energy dependence of the RIXS spectrum measured on PrFeAsO at $q = (\pi, \pi)$. The top and bottom panels are, respectively, centered around the resonance of the CT and dd features. The vertical shift between the spectra in the top panel is half of that in the bottom panel. (b) Fe K edge measured in the partial fluorescence yield on PrFeAsO and PrFeAsO_{0.7} for both $\varepsilon//a$ and $\varepsilon//c$ incident photon polarization conditions. (c) Fe $3d$ and As $4p$ density of states calculated for LaFeAsO.

inelastic features are seen in Fig. 1(a), which show Raman-like behavior, i.e., stay at constant energy loss, around 1.5 and 4.0 eV, respectively. In contrast, the strong spectral weight that grows above 6 eV at $E_i = 7119$ eV follows a slope-one linear dependence with E_i and is assigned to the tail of the $K\beta_{2,5}$ ($3d \rightarrow 1s$) emission line.

It is worth remarking that the intrinsic intensity of the RIXS features of PrFeAsO is ~ 40 times weaker than the much-studied cuprates and nickelates using a similar setup. In part, this is because of the itinerant nature of the Fe $3d$ electrons, which reduces their interaction with the $1s$ core-hole in the RIXS intermediate state, and thus reduces the probability for valence-band excitations. Further, the onsite p - d hybridization, allowed by the absence of a center of symmetry at the tetrahedral Fe site, is expected to enhance the $K\beta_{2,5}$ fluorescence cross-section, at the expense of the RIXS cross-section. We note, however, that, in spite of the low intensity, our observation of charge excitations marks a major step forward compared with studies reported at the Fe- L edge of the 1111, 122, ³ and 11 systems ⁴ where any Raman features were seemingly hidden by the strong fluorescence background.

Having observed charge excitations in the face of strongly fluorescence-dominated data, the way is now cleared for their identification. Based on calculations of the Fe $3d$ and As $4p$ densities of states (DOS) of LaFeAsO shown in Fig. 1(c), we assign the experimental Raman features observed at 1.5 and 4.0 eV to interband transitions between occupied Fe $3d$ states and unoccupied states of dominant Fe $3d$ character, and between occupied As $4p$ states and unoccupied states of dominant Fe $3d$ character, respectively. We hereafter refer to these 1.5- and 4.0-eV features as dd interband (dd) and charge transfer (CT) excitations, respectively.

We now take a close look at the momentum dependence of the RIXS spectrum of PrFeAsO, shown in Fig. 2(c) for high symmetry points of the folded Brillouin zone (two Fe atoms in the unit cell) represented in Fig. 2(a). These data

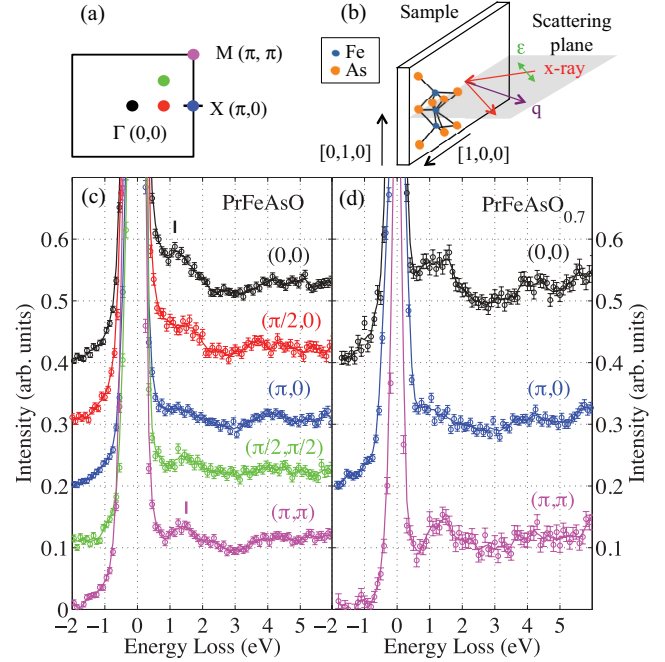


FIG. 2. (Color online) (a) Two-dimensional folded Brillouin zone. The colored dots correspond to the color of the plots in panels (c) and (d). (b) Scattering geometry with the incident photon polarization ε parallel to the ac plane. Momentum dependence of the RIXS spectrum of PrFeAsO (c) and PrFeAsO_{0.7} (d). The circles are the raw data and the lines are three-point smoothed spectra. Data are shifted vertically for clarity. Vertical ticks indicate the energy position of the dd feature at $(0,0)$ and (π, π) .

were measured at $E_i = 7121$ eV, which corresponds to the maximum of the resonance, and where the $K\beta_{2,5}$ emission is at sufficiently high energy loss to not overlap with the energy range of interest. While there is no sizable dispersion for the CT excitation, the dd feature is found to be weakly dispersive. Unless strong electron correlations come into play, the momentum dependence of the RIXS spectrum can be conveniently thought of as a measure of the momentum-resolved joint DOS (JDOS).⁷ The momentum dependence of the dd peak is, therefore, expected to correlate with the dispersion of all five Fe d bands, the tangle of which constitutes most of the DOS in the vicinity of the Fermi level.⁸ Thus, one would expect only a weak overall dispersion of the dd feature. The momentum dependence of the RIXS spectrum of PrFeAsO_{0.7} is shown in Fig. 2(d). Although the statistics do not allow a detailed comparison with PrFeAsO, we can conclude that the main spectral features are similar for both compounds: A momentum-independent CT feature and a dd interband excitation whose center of mass slightly shifts toward higher energies from $(0,0)$ to (π, π) and decreases in intensity around $(\pi, 0)$.

In order to gain insight on the nature of the observed charge excitations, we have carried out a theoretical analysis of the RIXS spectrum using a 16-band dp model.⁹ The antiferromagnetic ground state is described by the Hartree-Fock (HF) theory and electron correlations in the excitation process are taken into account within the random-phase approximation (RPA). Previous studies showed the quantitative reliability of our theoretical framework within the RPA.¹⁰⁻¹² The scattering

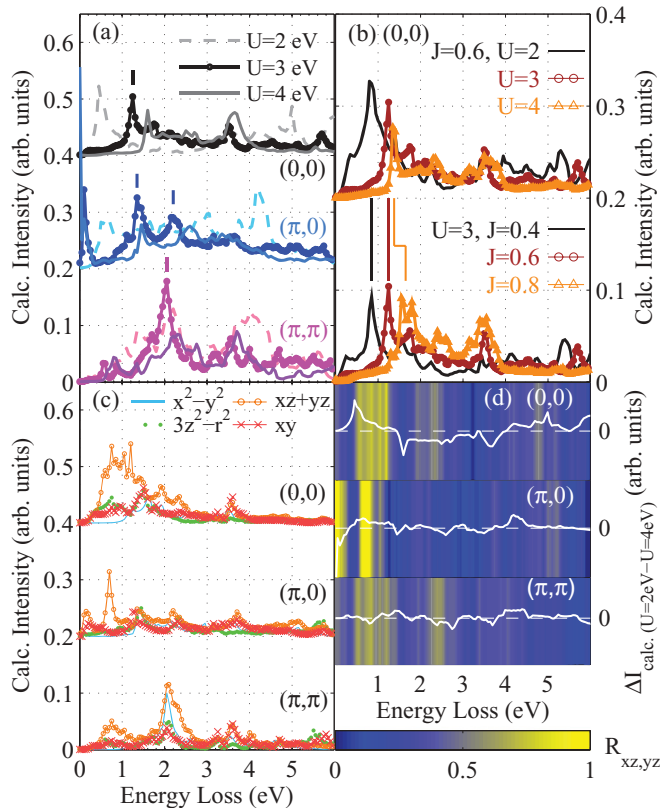


FIG. 3. (Color online) (a) RIXS spectra calculated at $q = (0,0)$, $(\pi,0)$, and (π,π) for $U = 2, 3$, and 4 eV and $J = 0.2 \times U$. (b) U and J dependencies of the RIXS spectrum calculated at $q = (0,0)$. (c) Diagonal orbital excitations calculated for $U = 3$ eV. (d) Difference between the momentum-resolved, area-normalized spectra calculated for $U = 2$ and 4 eV (white line) and intensity ratio of the diagonal transitions of xz, yz orbitals to the sum of the diagonal transitions of all five d orbitals for $U = 3$ eV (color bars).

of the Fe $3d$ electrons by the $1s$ core-hole is treated within the Born approximation. While our analysis does not take into account the multiple scattering between the core hole and the excited electron in the intermediate state, we note that the inclusion of this multiple scattering was previously shown to only have little effect on the calculated RIXS spectral shape and virtually no effect on the peak energies.¹³

Figure 3(a) shows the momentum-resolved spectra calculated for intraorbital Coulomb repulsion $U = 2, 3$, and 4 eV, with the interorbital Coulomb repulsion $U' = 0.6 \times U$ and Hund's coupling $J = 0.2 \times U$. The calculated spectra show an appreciable sensitivity to variation in correlations in their low-energy region, especially at $(0,0)$ where the energy position of the dd feature E_{dd} increases in a nearly linear fashion with U . Interestingly, a similar dependence on U was reported for the RIXS excitation between the lower and upper Hubbard bands in the Mott insulator NaV_2O_5 .¹⁴ This surprising observation provides strong evidence for the importance of the electron correlations effects in the pnictides and opens a way for a quantitative determination of U and J through a comparison between the energy position of the calculated and experimental dd peaks. In Fig. 4, we carry out such a comparison, where we have subtracted off the elastic line, obtained from a spectrum measured off resonance at

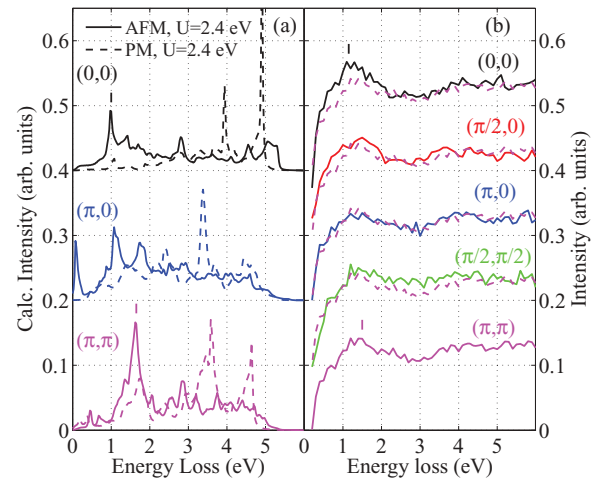


FIG. 4. (Color online) (a) RIXS spectra calculated for the anti-ferromagnetic (solid line) and the paramagnetic (dashed line) ground states, for $U = 2.4$ eV and bandwidth renormalized by a factor of 0.8. (b) Experimental RIXS spectra for PrFeAsO after subtraction of the elastic line. The spectrum measured at $q = (\pi, \pi)$ (dashed magenta) is overlaid with the spectra measured at other momenta. In both panels, vertical ticks indicate the energy position of the dd feature at $(0,0)$ and (π, π) .

$E_i = 7137$ eV. From this comparison, we find that although a good agreement can be obtained at $(0,0)$ for $U = 3$ eV ($J = 0.6$ eV), the energy of the calculated dd peaks at (π, π) is slightly too high. An improved match with experiment is obtained after renormalization of the theoretical bandwidth and U by a factor 0.8 [cf. Fig. 4(a)], thus yielding $U = 2.4$ eV ($J = 0.48$ eV). Our constraint on the value of U is consistent with the previous estimates for the 1111 system reported so far ranging between about 2 and 4 eV.^{15–18}

Now that we have determined the (U, J) combination with $J = 0.2 \times U$ for PrFeAsO , we look at the dependencies of the calculated spectrum on U and J for variations in U of ± 1 eV and J of ± 0.2 eV, in order to separately assess the respective roles of U and J . The results are shown in Fig. 3(b) for values of J ranging between 0.4 and 0.8 eV and U between 2 and 4 eV, with $U' = 0.6 \times U$. We make two main observations. First, decreasing J by 0.2 eV ($U = 3$ eV, $J = 0.4$ eV) or by 1 eV ($U = 2$ eV, $J = 0.6$ eV) yields the same value of $E_{dd} = 0.8$ eV. Further, increasing J by 0.2 eV ($U = 3$ eV, $J = 0.8$ eV) results in $E_{dd} = 1.7$ eV, which is higher than $E_{dd} = 1.3$ eV obtained by increasing U by 1 eV ($U = 4$ eV, $J = 0.6$ eV). These results stress the peculiar sensitivity of the RIXS spectrum to the value of J , which reflects the importance of Hund's coupling in the electron correlation of PrFeAsO , a consequence of the multiorbital electronic structure of the 1111 pnictide.¹

The orbital composition of the RIXS spectrum can be derived from the calculated diagonal transitions (i.e., for which the initial and final orbital states are identical), which account for most of the RIXS spectral weight. Such calculations are shown in Fig. 3(c) for $U = 3$ eV. The intensity ratio between the diagonal transitions of xz, yz character and the sum of the diagonal transitions for all five d orbitals, $R_{xz, yz}$, is plotted as color bars in Fig. 3(d). For all three momenta, the dd feature

is seen to largely arise out of xz, yz diagonal transitions for energies up to ~ 1.2 eV and then evolves into a blend of diagonal transitions of all five d orbitals at higher energies. The dd feature, therefore, straddles two ranges of distinct orbital composition.

We next address the interplay between electron correlation and the multiorbital effects. To this end, we consider the difference between the spectra calculated for $U = 2$ eV and for $U = 4$ eV, normalized in intensity to their respective area and shown as $\Delta I_{\text{calc.}(U=2\text{eV}-U=4\text{eV})}$ in Fig. 3(d). This illustrates the correlation-induced spectral weight (SW) transfer. We overlay it with the color bars of $R_{xz,yz}$ for the medium value $U = 3$ eV in Fig. 3(d). An examination of this plot, along with the calculated RIXS spectra in Fig. 3(a), reveals a close correspondence across the $(0,0)$ - $(\pi,0)$ - (π,π) sequence between the weakening of the low-energy xz, yz interband excitations and that of the correlation-induced shift of SW. Most notably, at (π,π) where the dd feature mostly gains intensity from the higher-energy (~ 2 eV) multiorbital transitions, there is no sizable SW shift as U is increased from 2 to 4 eV. This smaller sensitivity to correlations of the higher-energy, multiband excitations compared with that of the xz, yz ones points to strongly orbital-dependent correlation effects in PrFeAsO_{1-y} . In view of the strong similarities in the electronic structure within the 1111 family, we expect such effects to carry over across the REFeAsO (RE = rare-earth) series.

Next, we discuss the effect of the AFM correlations on the RIXS spectrum. The spectrum calculated for the paramagnetic (PM) ground state is shown in Fig. 4(a) along with the spectrum for the AFM ground state, both obtained for $U = 2.4$ eV. Surprisingly, the dd feature is nearly absent in the calculated spectrum of the PM ground state at $(0,0)$ and substantially weaker, compared with the AFM spectrum, at $(\pi,0)$ and (π,π) . These dramatic changes can be traced to the AFM-induced modifications of the band structure,¹⁹ as band folding is expected to result in a strong increase of the RIXS dd diagonal transitions, particularly at $(0,0)$. Remarkably, no decrease in the intensity of the dd feature is found in the experimental spectrum of $\text{PrFeAsO}_{0.7}$ compared with PrFeAsO for all three

measured momenta. Also, the dd feature for $\text{PrFeAsO}_{0.7}$ is not weaker at $(0,0)$ than at $(\pi,0)$ and (π,π) . These observations suggest that short-range AFM correlations are retained in the superconducting regime, even at optimal doping level. This is consistent with the observation of spin fluctuations in the optimally electron-doped 1111 system $\text{LaFeAsO}_{1-x}\text{F}_x$ using inelastic neutron scattering.²⁰

In summary, we have successfully observed charge-excitation features in the RIXS spectrum of an iron pnictide, PrFeAsO_{1-y} ($y = 0, 0.3$). Calculations based on a 16-band dp model best reproduce the momentum dependence of the experimental dd interband feature for $U = 2.4$ eV and $J = 0.48$ eV, which confirms that the 1111 pnictides are moderately correlated. The dd interband transitions are found to be xz, yz dominated and highly sensitive to correlations below ~ 1.2 eV, while multiorbital and poorly sensitive to correlations above ~ 1.2 eV. Such remarkable orbital-dependent properties at high energies lend support to theoretical models that suggest that superconductivity in the iron pnictides is induced by orbital fluctuations.²¹ Furthermore, the fact that the dd interband excitations, while predicted to nearly vanish for the nonmagnetic ground state at $(0,0)$, are observed in the superconductor, too, shows that local antiferromagnetic correlations survive in the superconducting state.

The authors are grateful to Y. Yanagi, Y. Yamakawa, and Y. Ono for sharing valuable information on the electronic structure. We thank H. Eisaki and A. Iyo for technical assistance with the crystal growth. This work is supported by a Grant-in-Aid for Specially Promoted Research 17001001 from the Ministry of Education, Culture, Sports, Science and Technology, Japan, and JST TRIP. Use of the Advanced Photon Source was supported by the US DOE under Contract No. DE-AC02-06CH11357. We thank NSRRC, Taiwan, for providing us beam time for preliminary experiments at BL12XU/SPring-8. Work at University of Toronto was supported by NSERC. Work at Brookhaven was supported by the US DOE, Division of Materials Science, under Contract No. DE-AC02-98CH10886.

*jarrige@bnl.gov; present address: National Synchrotron Light Source II, Brookhaven National Laboratory, Upton, New York 11973, USA.

†Present address: CROSS, Tokai, Naka, Ibaraki 319-1106, Japan.

¹L. de' Medici, *Phys. Rev. B* **83**, 205112 (2011).

²A. Liebsch, *Phys. Rev. B* **84**, 180505(R) (2011).

³W. L. Yang *et al.*, *Phys. Rev. B* **80**, 014508 (2009).

⁴J. N. Hancock *et al.*, *Phys. Rev. B* **82**, 020513(R) (2010).

⁵M. Ishikado *et al.*, *Physica C* **470**, S322 (2010).

⁶D. J. Singh and M.-H. Du, *Phys. Rev. Lett.* **100**, 237003 (2008).

⁷Y.-J. Kim, J. P. Hill, H. Yamaguchi, T. Gog, and D. Casa, *Phys. Rev. B* **81**, 195202 (2010).

⁸S. Ishibashi *et al.*, *J. Phys. Soc. Jpn.* **77**, 053709 (2008).

⁹Y. Yanagi, Y. Yamakawa, and Y. Ōno, *Phys. Rev. B* **81**, 054518 (2010).

¹⁰M. Takahashi, J. I. Igarashi, and T. Nomura, *Phys. Rev. B* **75**, 235113 (2007).

¹¹T. Semba, M. Takahashi, and J. I. Igarashi, *Phys. Rev. B* **78**, 155111 (2008).

¹²T. Nomura and J. I. Igarashi, *Phys. Rev. B* **71**, 035110 (2005).

¹³J. I. Igarashi, T. Nomura, and M. Takahashi, *Phys. Rev. B* **74**, 245122 (2006).

¹⁴G. P. Zhang, T. A. Callcott, G. T. Woods, L. Lin, B. Sales, D. Mandrus, and J. He, *Phys. Rev. Lett.* **88**, 077401 (2002).

¹⁵K. Haule, J. H. Shim, and G. Kotliar, *Phys. Rev. Lett.* **100**, 226402 (2008).

¹⁶M. Aichhorn, L. Pourovskii, V. Vildosola, M. Ferrero, O. Parcollet, T. Miyake, A. Georges, and S. Biermann, *Phys. Rev. B* **80**, 085101 (2009).

¹⁷V. I. Anisimov *et al.*, *J. Phys.: Condens. Matter* **21**, 075602 (2009).

¹⁸T. Miyake *et al.*, *J. Phys. Soc. Jpn.* **79**, 044705 (2010).

¹⁹Z. P. Yin and W. E. Pickett, *Phys. Rev. B* **81**, 174534 (2010).

²⁰S. Wakimoto *et al.*, *J. Phys. Soc. Jpn.* **79**, 074715 (2010).

²¹See, for example, H. Kontani and S. Onari, *Phys. Rev. Lett.* **104**, 157001 (2010).